Journal of
*Composites Science*

MDPI

*Article*

# Simplified Approach for the Seismic Assessment of Existing X Shaped CBFs: Examples and Numerical Applications

**Rosario Montuori [1], Elide Nastri [2], Vincenzo Piluso [2] and Paolo Todisco [2,*]**

[1] Department of Pharmacy, University of Salerno, 84084 Fisciano, SA, Italy; r.montuori@unisa.it
[2] Department of Civil Engineering, University of Salerno, 84084 Fisciano, SA, Italy; enastri@unisa.it (E.N.); v.piluso@unisa.it (V.P.)
* Correspondence: ptodisco@unisa.it

**Abstract:** The capacity of a structure can be assessed using inelastic analyses, requiring sophisticated numerical procedures such as pushover and incremental dynamic analyses. A simplified method for the evaluation of the seismic performance of steel Concentrically Braced Frames (CBFs) to be used in everyday practice and the immediate aftermath of an earthquake has been recently proposed. This method evaluates the capacity of an existing building employing an analytical trilinear model without resorting to any non-linear analysis. The proposed methodology has been set up through a large parametric analysis, carried out on 420 frames designed according to three different approaches: the first one is the Theory of Plastic Mechanism Control (TPMC), ensuring the design of structures showing global collapse mechanisms (GCBFs), the second one is based on the Eurocode 8 design requirements (SCBFs), and the third is a non-seismic design, based on a non-seismic design (OCBFs). In this paper, some examples of the application of this simplified methodology are proposed with references to structures that are supposed to exhibit global, partial, and soft storey mechanisms.

**Keywords:** CBF; pushovers; capacity; performances; vulnerability; simplified methods



**Citation:** Montuori, R.; Nastri, E.; Piluso, V.; Todisco, P. Simplified Approach for the Seismic Assessment of Existing X Shaped CBFs: Examples and Numerical Applications. *J. Compos. Sci.* **2022**, *6*, 62. https://doi.org/10.3390/jcs6020062

Academic Editor: Francesco Tornabene

Received: 27 January 2022
Accepted: 16 February 2022
Published: 18 February 2022



## 1. Introduction

Recent seismic events have underlined the high seismic vulnerability of a large part of the built heritage and, consequently, the importance of its safeguarding [1–21]. With a view to a large-scale classification of the existing buildings in terms of seismic vulnerability, the definition of a simplified methodology that allows for an evaluation of the seismic performance without resorting to analyses that require high numerical complexities, such as pushover analysis and incremental dynamic analysis, plays an important role [22–31]. These procedures also do not result in seismic classification and code liability, being strongly influenced by the software used to develop them, nor the modeling of the members, which is characterized by numerous variables that are difficult to standardize [32–35].

Consequently, a completely analytical simplified model allowing us to univocally control these complexities is introduced for steel Concentrically Braced Frames (CBFs) [36].

The methodology is set up for general use. It is based on the use of elastic analysis combined with rigid plastic analysis for both CBFs and MRFs. The difference lies in the definition of some characteristic points. The capacity curve is represented through a trilinear approximation. In particular, CBFs are characterized by presenting a second elastic branch with reduced stiffness for the buckling of the compressed diagonals, whereas MRFs have a horizontal branch due to the plastic redistribution capacity typical of the structural type.

The performance-based assessment procedure is herein applied to some study cases in order to testify both the ease and speed of the application of the method. This procedure consists of identifying some characteristic points associated with target performance objectives on a trilinear simplified capacity curve [37,38]. These points correspond to different limit states.

The procedure was validated by a wide parametric analysis on 420 CBFs, designed according to three different approaches, i.e., for horizontal loads only (OCBFs), according to the provisions of Eurocode 8 (SCBFs), and in accordance with the theory of plastic mechanism control (GCBFs). The design according to three approaches was carried out to ensure a database of frames capable of covering the design philosophies of recent decades. It is known that structures designed without prescriptions aimed at controlling the collapse mechanism are used to exhibit soft storey mechanisms, unlike structures designed according to Eurocode 8, which are capable of avoiding these types of mechanisms without, however, guaranteeing the development of global collapse mechanisms, which is obtainable instead with the use of the TPMC approach. For the designed structures, pushover analyses were carried out to calibrate the proposed analytical relationships and, thus, to ensure a wide applicability of the method.

The comparison in terms of capacity and demand can be made according to two alternative approaches: the one proposed by Eurocode 8 [39] and the one proposed by Nassar and Krawinkler [40]. The former exploits the concept of the ADRS spectrum, whereas the latter has the benefit of having an easier applicability because it does not distinguish between low and high periods of vibration. In the following, the main model equations are reported and described.

## 2. Fundamental Equations of the Trilinear Model

For the definition of the trilinear capacity curve, elastic analysis and second-order rigid-plastic analysis are necessary, without resorting to complex static or dynamic non-linear analyses [41–44].

This tool then allows for a quick representation of the capacity curve through the intersection of three branches (Figure 1), whose equations are shown below.

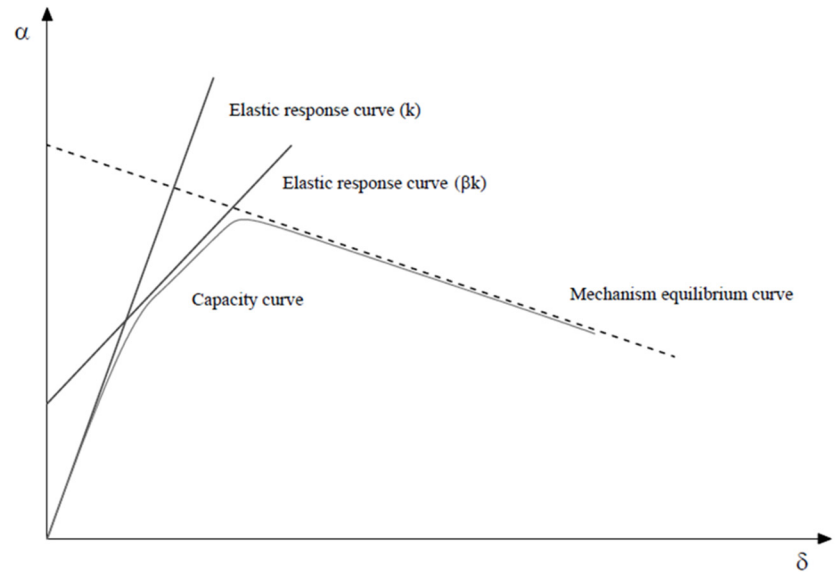


**Figure 1.** Trilinear approximation of the capacity curve for CBFs.

In the proposed model, the first branch of the curve is represented by the elastic response curve; the second one is defined as an elastic response curve with reduced stiffness, due to the buckling of the compressed diagonals; and the third (softening branch) is represented by the collapse mechanism equilibrium curve of the given structure, influenced by the second-order effects [45–51].

The mechanism equilibrium curve can be obtained by equating the virtual internal work of the dissipative zones with the virtual external work of the structure, considering second-order effects. The most likely collapse mechanism can be identified as the one

corresponding to the lower mechanism equilibrium curve, in a range of displacements compatible with the local ductility resources.

The equations of the three identified branches in the α-δ plane (horizontal force multiplier–top sway displacement) are reported below:

- Elastic response curve:

$$\alpha = \frac{1}{\delta_1}\delta \tag{1}$$

In addition, in order to check the precision of the model, a calibration procedure has been carried out on the well-known Merchant–Rankine formula, which is able to define the maximum multiplier of the structure.

The equations of the three identified branches in the α-δ plane (horizontal force multiplier–top sway displacement) are here reported:

- Elastic response curve ($k$):

$$\alpha_{b,s} = \alpha_A = \frac{1}{\delta_1}\delta_A \tag{2}$$

- Elastic response curve with reduced stiffness ($k'$):

$$\alpha_{e,2} = \alpha_A + K'(\delta - \delta_A) \tag{3}$$

where

$$K' = \beta K \tag{4}$$

$$\beta = 1 - \left(\frac{P_{y.1} - P_{crit.1}}{P_{y.1}}\right) 0.5 \cdot \frac{H_0}{H} \tag{5}$$

$\left(\frac{P_y - P_{crit}}{P_y}\right)$ represents the relative difference between the axial resistance in tension and the axial buckling resistance of the diagonal members. Reference is made to the members of the first storey.

- Mechanism equilibrium curve:

$$\alpha = \alpha_0 - \gamma_s(\delta - \delta_y) \tag{6}$$

The relationships for the evaluation of the collapse multipliers for each possible collapse mechanism are reported:

- For global collapse mechanism:

$$\alpha_0^{(g)} = \frac{\sum_{k=1}^{n_s}\sum_{j=1}^{n_b} W_{d.jk}}{\sum_{k=1}^{n_s} F_k h_k} \tag{7}$$

- For type-1 mechanism:

$$\alpha_{0.i_m}^{(1)} = \frac{\sum_{k=1}^{i_m-1}\sum_{j=1}^{n_b} W_{d.jk} + \sum_{i=1}^{n_c} M_{c.ii_m}}{\sum_{k=1}^{i_m} F_k h_k + h_{i_m}\sum_{k=i_m+1}^{n_s} F_k}; \quad i_m = 1, 2, \ldots, n_{s-1} \tag{8}$$

$$\alpha_{0.n_s}^{(1)} = \alpha_0^{(g)}; \quad i_m = n_s \tag{9}$$

- For type-2 mechanism

$$\alpha_{o.i_m}^{(2)} = \frac{\sum_{k=i_m}^{ns}\sum_{j=1}^{n_b} W_{d.jk} + \sum_{i=1}^{n_c} M_{c.ii_m}}{\sum_{k=i_m}^{n_s} F_k \cdot (h_k - h_{i_m-1})}; \qquad i_m = 2, 3, \ldots, n_s \tag{10}$$

- For type-3 mechanism:

$$\alpha_{0.i_m}^{(3)} = \frac{2 \cdot \sum_{i=1}^{n_c} M_{c.ii_m} + \sum_{j=1}^{n_b} W_{d.ji_m}}{(h_{i_m} - h_{i_m-1}) \cdot \sum_{k=i_m}^{n_s} F_k}; \qquad 2 \le i_m < n_s \tag{11}$$

$$\alpha_{0.n_s}^{(3)} = \frac{\sum_{i=1}^{n_c} M_{c.in_s} + \sum_{j=1}^{n_b} W_{d.jn_s}}{(h_{n_s} - h_{n_s-1}) \cdot F_{n_s}}; \qquad i_m = n_s \tag{12}$$

$$\alpha_{0.1}^{(3)} = \frac{\sum_{i=1}^{n_c} M_{c.i1} + \sum_{j=1}^{n_b} W_{d.j1}}{h_1 \cdot \sum_{k=1}^{n_s} F_k}; \qquad i_m = 1 \tag{13}$$

The internal work $W_{d.jk}$ due to the diagonal members of $j$-th bay of $k$-th storey, is given for a unit virtual rotation of base hinges of columns and is defined as follows:

$$W_{d.jk} = N_{t.jk} \cdot e_{t.jk} + N_{c.jk}(\delta_u) \cdot e_{c.jk} \tag{14}$$

The axial force $N_{c.jk}(\delta_u)$ is defined through the first three branches of the Georgescu's model [40,41]:

- OA branch:

$$P = \frac{EA}{L}\delta_{OA} = K_d \delta_{OA} \quad with\ P\ limited\ to\ P_{crit} \tag{15}$$

- AB branch:

$$f_{tB} = \frac{M_{pl}}{P_{crit}}\left(1 - \frac{P_{crit}}{P_y}\right) \tag{16}$$

$$\delta_B = -\frac{P_{crit} L}{EA} + \frac{\pi^2}{4L}\left({f_{tB}}^2 - {f_0}^2\right) \tag{17}$$

- BC branch:

$$f_t = \frac{M_{pl}}{P}\left(1 - \frac{P}{P_y}\right) \ with\ P\ generic < P_{crit} \tag{18}$$

$$f_0 = \delta_{BC} = -\frac{PL}{EA} + \frac{\pi^2}{4L}\left({f_t}^2 - {f_0}^2\right) \tag{19}$$

The link describing the monotonic behaviour of the diagonals is completed by defining the behaviour in tension, adding the branches OF and FG, as reported in Figure 2.

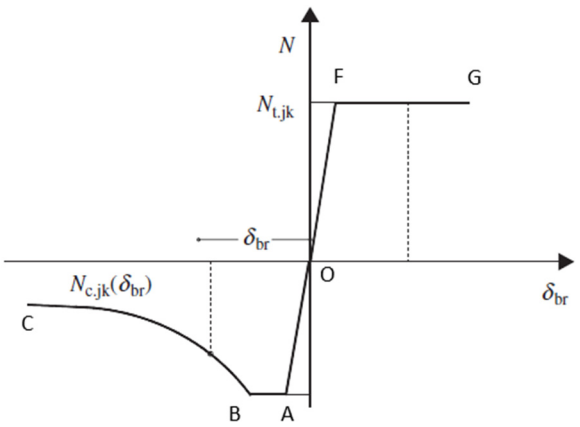


**Figure 2.** Monotonic behaviour for diagonal members in compression and tension.

The slopes of the equilibrium curve for each type of mechanism can be defined as follows:

- For the global collapse mechanism:

$$\gamma^{(g)} = \frac{1}{h_{n_s}} \frac{\sum_{k=1}^{n_s} V_k h_k}{\sum_{k=1}^{n_s} F_k h_k} \tag{20}$$

- For the type-1 mechanism:

$$\gamma_{i_m}^{(1)} = \frac{1}{h_{i_m}} \frac{\sum_{k=1}^{i_m} V_k h_k + h_{i_m} \sum_{k=i_m+1}^{n_s} V_k}{\sum_{k=1}^{i_m} F_k h_k + h_{i_m} \sum_{k=i_m+1}^{n_s} F_k} \tag{21}$$

- For the type-2 mechanism:

$$\gamma_{i_m}^{(2)} = \frac{1}{h_{n_s} - h_{i_m-1}} \frac{\sum_{k=i_m}^{n_s} V_k (h_k - h_{i_m-1})}{\sum_{k=i_m}^{n_s} F_k (h_k - h_{i_m-1})} \tag{22}$$

- For the type-3 mechanism:

$$\gamma_{i_m}^{(3)} = \frac{1}{h_{i_m} - h_{i_m-1}} \frac{\sum_{k=i_m}^{n_s} V_k}{\sum_{k=i_m}^{n_s} F_k} \tag{23}$$

- Maximum multiplier according to calibrated Merchant–Rankine formula [52,53]:

$$\alpha_{max} = \frac{\alpha_0}{1 + \Psi_{CBF} \alpha_0 \gamma_s \delta_1} \tag{24}$$

where

$$\Psi_{CBF} = a + b \xi_{CBF} \tag{25}$$

$$\xi_{CBF} = \frac{\sum_{n_{b_c}} \frac{EA_{diag}}{L_{diag}} \cdot \frac{1}{1+(L_b/h)^2}}{\sum_{n_c} \frac{EI_c}{h^3}} \tag{26}$$

The use of Equation (4) is proposed by assuming, for the coefficient $\Psi$, the following relation considering GCBFs and SCBFs:

$$\Psi_{CBF} = 1.00421 + 0.10265\ \xi_{CBF} \tag{27}$$

The coefficient $\Psi_{CBF}$ has been derived also considering separately GCBFs and SCBFs. For global concentrically braced frames,

$$\Psi_{CBF} = 1.410677 + 0.294433\ \xi_{CBF} \tag{28}$$

whereas, for special concentrically braced frames,

$$\Psi_{CBF} = 0.18799 + 0.11338\ \xi_{CBF} \tag{29}$$

The characteristic performance points of the capacity curve (points A, B, C, D of Figure 3) have been identified on the trilinear model. The points are associated with specific limit states [50], provided by codes, identifying the achievement of a specific performance level [47,54–56].

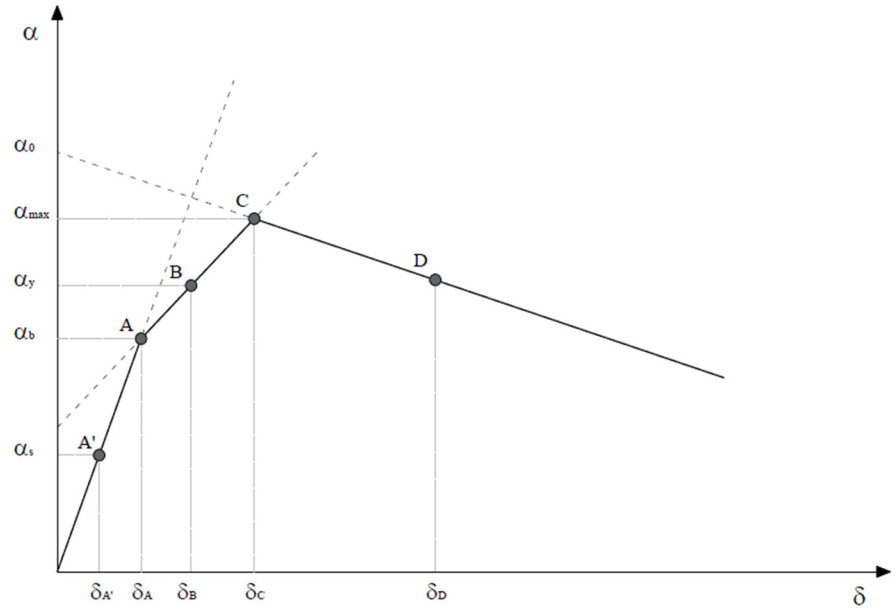


**Figure 3.** Characteristic performance points.

- Point A—"Fully Operational"

$$\alpha_{b,s} = \alpha_A = \frac{1}{\delta_1}\delta_A \tag{30}$$

- Point B—"Operational"

$$\alpha_B = \alpha_A + K'(\delta_B - \delta_A)\,; \qquad \delta_B = \frac{\alpha_y - \alpha_A}{K'} + \delta_A \tag{31}$$

- Point C—"Life Safety"

$$\alpha_C = \alpha_0 - \gamma_s(\delta_C - \delta_y)\,; \qquad \delta_C = \frac{\alpha_0 - \alpha_A + K'\delta_A}{K' + \gamma_s} \tag{32}$$

This point is determined through the intersection of the second elastic branch with the softening branch, representative of the collapse mechanism equilibrium curve.

- Point D—"Near Collapse"

$$\delta_D = \delta_C + \varphi_{lim} \cdot H_0 \tag{33}$$

$$\delta_D = \delta_C + \left(\frac{\delta_{d,cp}}{h_i \cdot \cos\theta}\right) \cdot H_0 \tag{34}$$

The inelastic deformation capacity for compressed braces (Table 1) is expressed in terms of the axial deformation of the brace, as a multiple of the axial deformation of the brace corresponding to buckling load $\Delta_c$.

**Table 1.** Capacity in terms of axial deformation for braces in compression.

| | Limit State | | |
|---|---|---|---|
| **Class of Cross-Section** | **DL** | **SD** | **NC** |
| 1 | 0.25 $\Delta_C$ | 4.0 $\Delta_C$ | 6.0 $\Delta_C$ |
| 2 | 0.25 $\Delta_C$ | 1.0 $\Delta_C$ | 2.0 $\Delta_C$ |

For braces in tension (Table 2), the inelastic deformation capacity should be expressed in terms of the axial deformation of the brace as a multiple of the axial deformation of the brace at tensile yielding load Δt.

**Table 2.** Capacity in terms of axial deformation for braces in compression.

| Limit State | | |
|---|---|---|
| **DL** | **SD** | **NC** |
| 0.25 $\Delta_C$ | 7.0 $\Delta_C$ | 9.0 $\Delta_C$ |

## 3. Assessment Procedure in Terms of Spectral Accelerations According to ADRS Spectrum

The capacity–demand assessment procedure can be expressed through the ADRS spectrum. For each limit state, the spectrum $S_a - S_{De}$ will be be defined by means of the relationship $S_{De}(T) = S_a(T)(T/2\pi)^2$. With regard to the capacity, it is necessary to represent the performance points of the behavioral curve of the structure in the ADRS plane. Of these points, it will be necessary to obtain the displacements $d^*_{LS} = d_{LS}/\Gamma$.

The cases $T^* > T_C$ and $T^* < T_C$. If $T^* > T_C$ must be distinguished [48]. The capacity in terms of spectral acceleration, relative to the limit state considered, can be obtained as follows:

$$S_{aSL} = d^*_{LS}\omega^{*2}_0 \tag{35}$$

The demand is represented by the spectral acceleration provided by the code, for the specific limit state, in the case of the equivalent SDOF system with the equivalent period of vibration $T^*$.

For the assessment procedure, the inequality $S_{als} \geq S_a(T^*)$ must be satisfied.

If $T^* < T_C$ and $q > 1$, according to the equality of energy criteria, there is a different procedure to evaluate the capacity that leads to the anelastic spectrum:

$$F^*_{ls} = \frac{m^* S_a(T^*)}{q_{ls}} \tag{36}$$

$$q_{ls} = 1 + (\mu_{ls} - 1)\frac{T^*}{T_C} \tag{37}$$

$$S_{aSL} = q_{ls}\frac{F^*_{ls}}{m^*} \tag{38}$$

If $T^* < T_C$ and $q \leq 1$, it results in:

$$F^*_{SL} = m^* S_a(T^*) \tag{39}$$

$$S_{aSL} = \frac{F^*_{ls}}{m^*} \tag{40}$$

$$m^* = \sum_{k=1}^{n} m_{k\cdot k} \tag{41}$$

The checking is verified when the inequality $S_{als} \geq S_a(T^*)$ is satisfied.

## 4. Assessment Procedure in Terms of Spectral Accelerations According to Nassar and Krawinkler

In the framework of capacity–demand checking [52–58], an equivalent SDOF system replaces the MDOF actual system exploiting the modal participation factor Γ. The capacity curve is reported in a $F_b$-$d_c$ plane by multiplying $\alpha$ with the design base shear force. Then the capacity curve must be reduced through the modal participation factor and represented in a F*-d* plane. The demand is estimated according to the equivalent period $T^*$ and the

equivalent mass $m^*$ as reported by the European codes. The capacity in terms of spectral acceleration for the points A, B, C, D is defined as follows:

- Point A—"Fully Operational"

$$S_{aFO}(T^*) = \frac{F^*_{FO}}{m^*} \tag{42}$$

- Point B—"Operational"

$$S_{aO}(T^*) = \frac{F^*_{O}}{m^*} \tag{43}$$

- Point C—"Life Safety"

$$F^*_{LS} = m^* S_{aLS}(T^*) \tag{44}$$

$$S_{aLS}(T^*) = \frac{F^*_{LS}}{m^*} \tag{45}$$

- Point D—"Near Collapse"

$$S_{aNC}(T^*) = \frac{F^*_{NC}}{m^*} q_{NC} \tag{46}$$

$$q_{NC} = \frac{q_0}{\varphi} \tag{47}$$

$$q_0(\mu, T, \gamma_{=0}) = [c(\mu_{NC} - 1) + 1]^{1/c} \tag{48}$$

where $c = \frac{T^*}{1+T^*} + \frac{0.42}{T^*}$ and $\mu_{NC} = \frac{{d_{NC}}^*}{{d_O}^*}$

$$\varphi = \frac{1 + 0.62(\mu_{NC} - 1)^{1.45}\gamma}{(1 - \gamma)} \tag{49}$$

## 5. Numeric Examples

The simplified assessment procedure is applied to evaluate the capacity of three steel Concentrically Braced Frames designed according to three different approaches. Permanent loads $G_k$ are equal to 3.5 kN/m$^2$ wile live loads $Q_k$ equal to 3 kN/m$^2$. A frame tributary length of 6.00 m has been considered for the evaluation of gravitational loads acting on the beams. The steel used is S275.

A flowchart of the procedure is reported in Figure 4.

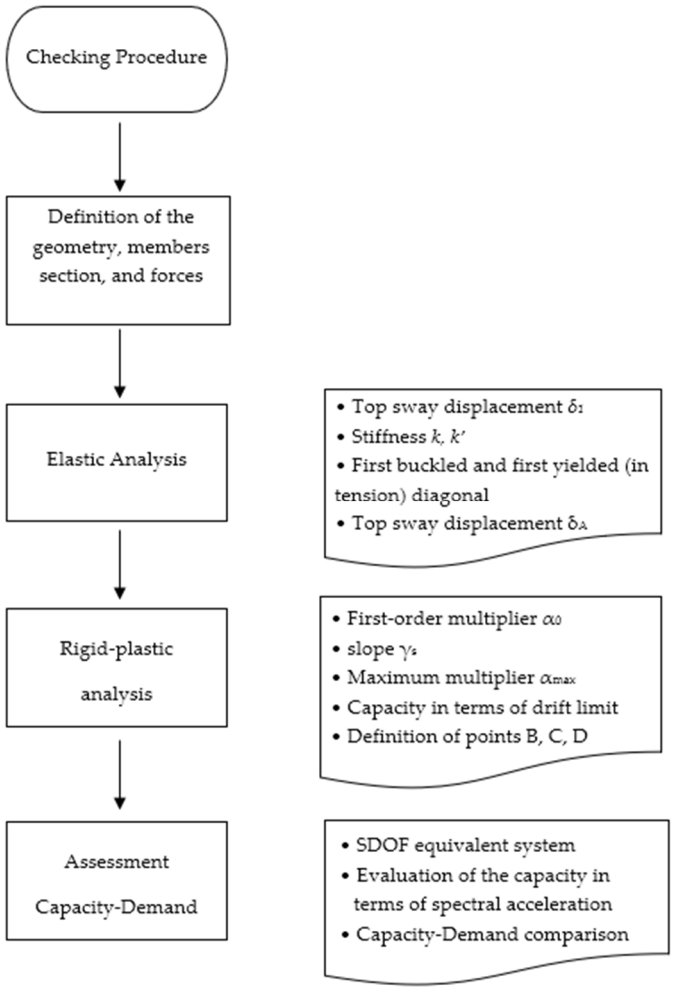


**Figure 4.** Flowchart of the procedure.

### *5.1. Global Concentrically Braced Frame*

Global concentrically braced frames are designed according to the TPMC. The beams, diagonals, and column sections are reported in Figure 5.

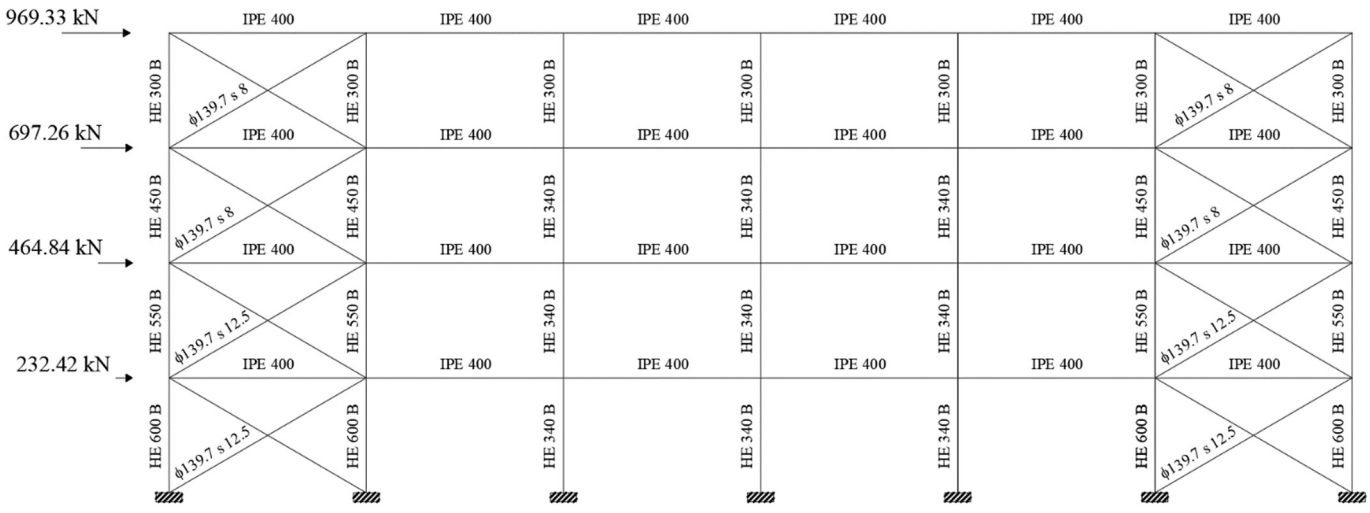


**Figure 5.** Diagram of the frame with indication of beams, diagonals, columns, and seismic forces (GCBF).

The trilinear capacity curve, showing the characteristic points of the model, is re-ported in Figure 6.

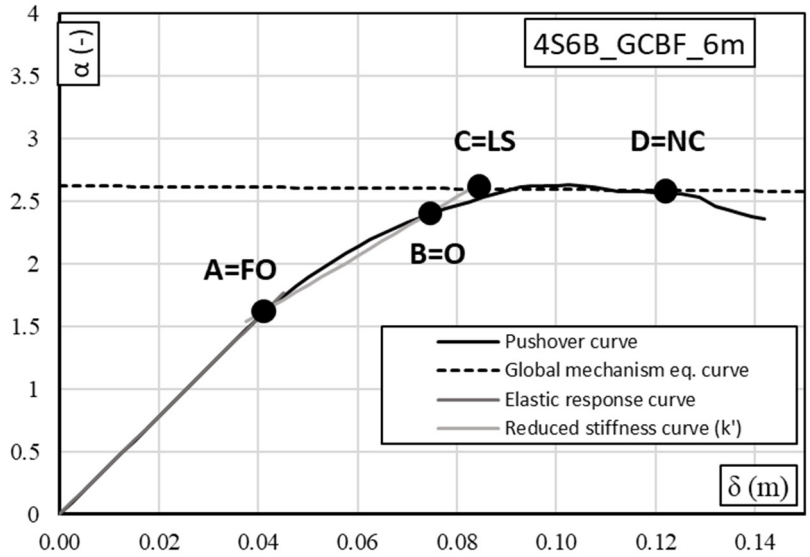


**Figure 6.** Trilinear model and characteristic points for the structure 4S6B_GCBF_6m 6.

Parameters obtained from the elastic analysis:

- $\delta_1(\alpha = 1) = 0.0255$ m;
- $K = 39.161$ m$^{-1}$;
- $K'$ =23.4964 m$^{-1}$;
- $\delta_A(1^{st}$ buckling$)$ =0.0426 m;
- $\alpha_A = k\delta_A$ =1.6577.

Parameters obtained from the rigid plastic analysis:

- $\alpha_0$ =2.598;
- $\gamma_s$ =0.285 m$^{-1}$;
- $\alpha = \alpha_0 - \gamma_s(\delta - \delta_y) \rightarrow \alpha = 2.598 - 0.285(\delta - 0.07438)$;
- $\alpha(\delta = 0) = \alpha_0 + \gamma_s\delta_y = 2.620$;
- $H_0 = 14\ m$ (global collapse mechanism).

Evaluation of the maximum multiplier through the calibrated Merchant–Rankine formula:

- $\alpha_{max} = \frac{\alpha_0}{1+\Psi_{CBF}\alpha_0\gamma_s\delta_1}$ =2.5058

  where

- $\Psi_{\mathrm{CBF}} = \mathrm{a} + \mathrm{b}\xi_{\mathrm{CBF}} = 1.41068 + 0.29443\ \xi_{CBF} = 1.698909$;
- with $\xi_{\mathrm{CBF}} = \frac{\sum_{n_{bc}} \frac{EA_{diag}}{L_{diag}} \cdot \frac{1}{1+(L_b/h)^2}}{\sum_{n_c} \frac{EI_c}{h^3}} = 1.945191$;
- consequently $\delta_{\mathrm{B}} = \frac{\alpha_y - \alpha_A}{K'} + \delta_A$ =0.07438;
- and $\delta_C = \frac{\alpha_0 - \alpha_A + K'\delta_A}{K' + \gamma_s} = 0.08163$.

According to the limitations given by Eurocode 8 for compressed diagonals at Near Collapse limit state ($\Delta_c \cdot 6$), the ultimate displacement is evaluated as:

- $\delta_D = \left(\frac{\delta_{d,cp}}{h_i \cdot \cos\theta}\right) \cdot H_0 = \left(\frac{0.026874}{3.5 \times 0.86378}\right) \times 14 = 0.12445\ m$

The checking procedures exploit the transformation of the MDOF system into an equivalent SDOF system through the participation factor of the main vibration mode Γ. For this reason, it is necessary to define:

- The eigenvector $\underline{\phi} = \{\phi_1, \phi_2, \phi_3, \phi_4\}$ that, assuming $\phi_k = \frac{F_k}{F_n}$, is:
  $\phi_1 = 0.2398$ $\phi_2 = 0.4795$ $\phi_3 = 0.7193$
  $\phi_4 = 1.00$
- The modal participation factor Γ:

$$\Gamma = \frac{\sum_{k=1}^{n} m_k \phi_k}{\sum_{k=1}^{n} m_k {\phi_k}^2} = 1.343$$

being

$$m_1 = 278.75 \times 10^3 \text{ kg } m_2 = 278.75 \times 10^3 \text{ kg } m_3 = 278.75 \times 10^3 \text{kg}$$
$$m_4 = 290.64 \times 10^3 \text{ k}$$

- The dynamic parameters of the equivalent SDOF system (Table 3).

**Table 3.** Dynamic parameters of the equivalent SDOF system (GCBF).

| $m^*$ [kg $10^3$] | $k^*$ [kN/m] | $\omega^*$ [rad/s] | $T^*$ [s] |
|---|---|---|---|
| **691.67** | **92,569.9** | **11.5688** | **0.5431** |

Consequently, the performance points of the capacity curve are defined in the planes $\alpha - \delta$, $F_b - d_c$, $F^* - D^*$, $S_a - S_D$ assessing the capacity in terms of accelerations for both Nassar & Krawinkler and ADRS spectrum approaches. In Tables 4 and 5 the results, based on the ADRS spectrum the Nassar & Krawinkler formulation, are respectively reported.

**Table 4.** ADRS spectrum approach (GCBF).

| | **FO** | **O** | **LS** | **NC** |
|---|---|---|---|---|
| F [kN] | 3918.52 | 5683.83 | 6086.44 | 6057.55 |
| F* [kN] | 2917.66 | 4232.08 | 4531.86 | 4510.35 |
| d [m] | 0.0426 | 0.0751 | 0.08163 | 0.12445 |
| d* [m] | **0.0317** | **0.0559** | **0.0608** | **0.0927** |
| $S_a$* [g] | **0.433** | **0.763** | **0.829** | **0.9803** |

**Table 5.** Nassar and Krawinkler approach (GCBF).

| | **FO** | **O** | **LS** | **$NC_0$** |
|---|---|---|---|---|
| F [kN] | 3918.52 | 5683.83 | 6086.44 | 6141.53 |
| F* [kN] | 2917.66 | 4232.08 | 4531.86 | 4572.88 |
| d [m] | 0.0426 | 0.0751 | 0.08163 | 0.12445 |
| d* [m] | **0.0317** | **0.0559** | **0.0608** | **0.0927** |
| μ [m] | - | - | - | **1.524** |
| $S_a$* [g] | **0.430** | **0.624** | **0.6679** | **1.0177** |

Seismic performance verification requires that, for each limit state, the inequality $S_{a.SL}(T^*)_{capacity} \geq S_{a.SL}(T^*)_{demand}$ is satisfied.

### *5.2. Special Concentrically Braced Frame*

Special concentrically braced frames are designed to fulfil the Eurocode 8 seismic provisions. The selected case study with the definition of the beam, diagonals, and column sections is reported in Figure 7.

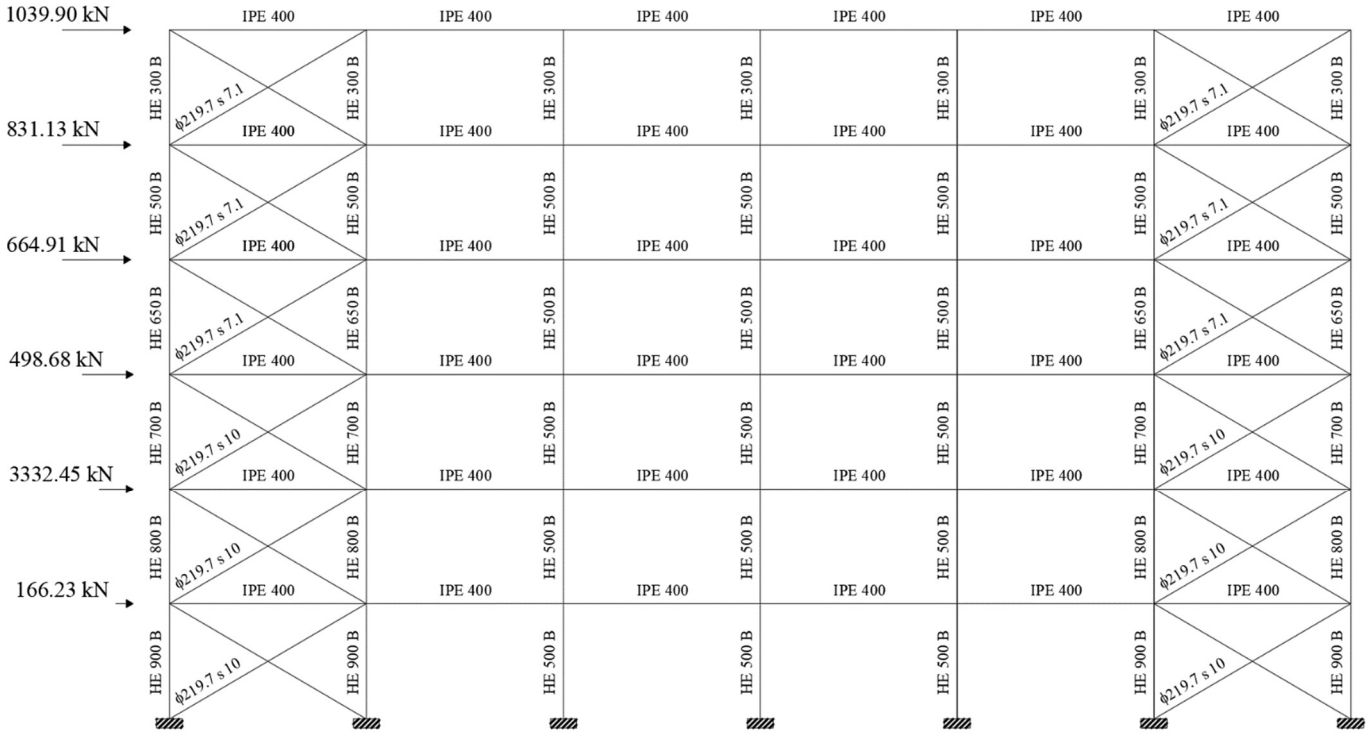


**Figure 7.** Diagram of the frame with indication of beams, diagonals, columns, and seismic forces (SCBF).

The trilinear capacity curve, showing the characteristic points of the model, is re-ported in Figure 8.

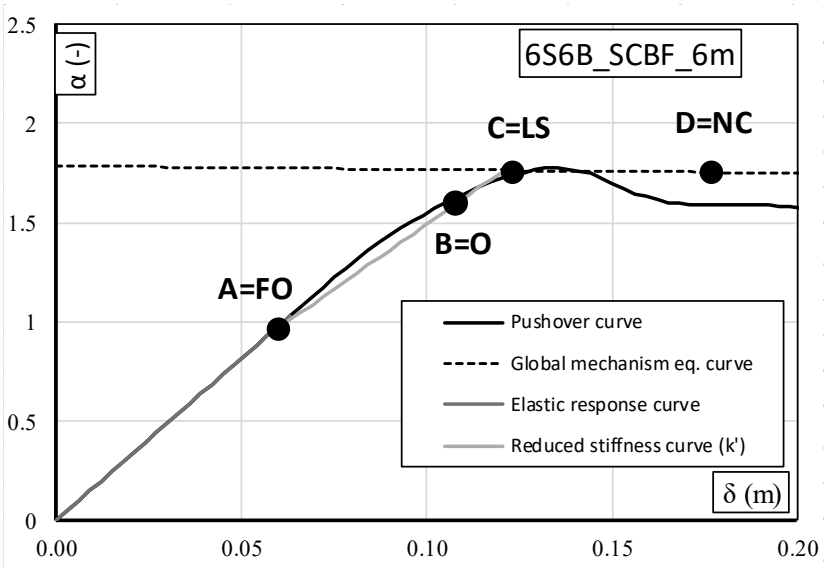


**Figure 8.** Trilinear model and characteristic points for the structure 6S6B_SCBF_6 m.

Parameters obtained from the elastic analysis:

- $\delta_1(\alpha = 1) = 0.06133$ m;
- $K = 16.305\ \mathrm{m}^{-1}$;
- $K' = 13.044\ \mathrm{m}^{-1}$;
- $\delta_A\left(1^{st}\ \text{buckling}\right) = 0.0571$ m;
- $\alpha_A = k\delta_A = 0.9311$.

Parameters obtained from the rigid plastic analysis:

- $\alpha_0$ =1.763;
- $\gamma_s$ =0.185 $m^{-1}$;
- $\alpha = \alpha_0 - \gamma_s(\delta - \delta_y) \rightarrow \alpha = 1.763 - 0.185(\delta - 0.1171)$;
- $\alpha(\delta = 0) = \alpha_0 + \gamma_s \delta_y = 1.785$;
- $H_0 = 21\ m$ (global collapse mechanism).

Evaluation of the maximum multiplier through the calibrated Merchant–Rankine formula:

- $\alpha_{max} = \frac{\alpha_0}{1+\Psi_{CBF}\alpha_0\gamma_s\delta_1}$ =1.7267

where

- $\Psi_{CBF} = a + b\xi_{CBF} = 1.00421 + 0.10265\ \xi_{CBF} = 1.05338$;
- With $\xi_{CBF} = \frac{\sum_{n_{b_c}} \frac{EA_{diag}}{L_{diag}} \cdot \frac{1}{1+(L_b/h)^2}}{\sum_{n_c} \frac{EI_c}{h^3}}$ = 0.47899;
- consequently $\delta_B = \frac{\alpha_y - \alpha_A}{K'} + \delta_A$ =0.1171;
- and $\delta_C = \frac{\alpha_0 - \alpha_A + K'\delta_A}{K' + \gamma_s} = 0.11922$.

According to the limitations given by Eurocode 8 for compressed diagonals at Near Collapse limit state ($\Delta_c \cdot 6$), the ultimate displacement is evaluated as:

- $\delta_D = \left(\frac{\delta_{d,cp}}{h_i \cdot \cos\theta}\right) \cdot H_0 = \left(\frac{0.026874}{3.5 \times 0.86378}\right) \times 21 = 0.18667\ m$

The checking procedures exploit the transformation of the MDOF system into an equivalent SDOF system through the participation factor of the main vibration mode Γ. For this reason, it is necessary to define:

- The eigenvector $\underline{\phi} = \{\phi_1, \phi_2, \phi_3, \phi_4, \phi_5, \phi_6\}$ that, assuming $\phi_k = \frac{F_k}{F_n}$, is:

$$\phi_1 = 0.1598\ \ \phi_2 = 0.3197\ \phi_3 = 0.4795$$
$$\phi_4 = 0.6394\ \phi_5 = 0.7992\ \phi_6 = 1.00$$

- The modal participation factor Γ:

$$\Gamma = \frac{\sum_{k=1}^{n} m_k \phi_k}{\sum_{k=1}^{n} m_k {\phi_k}^2} = 1.405$$

being

$$m_1 = 278.75 \times 10^3\ \text{kg}\ m_2 = 278.75 \times 10^3\ \text{kg}\ m_3 = 278.75 \times 10^3 \text{kg}$$
$$m_4 = 278.75 \times 10^3\ \text{kg}\ m_5 = 278.75 \times 10^3\ \text{kg}\ m_6 = 290.64 \times 10^3\ \text{kg}$$

- The dynamic parameters of the equivalent SDOF system (Table 6).

**Table 6.** Dynamic parameters of the equivalent SDOF system (SCBF).

| $m^*$ [kg $10^3$] | $k^*$ [kN/m] | $\omega^*$ [rad/s] | $T^*$ [s] |
|---|---|---|---|
| **959.01** | **57,610** | **7.75062** | **0.81067** |

Consequently, the performance points of the capacity curve are defined in the planes $\alpha - \delta$, $F_b - d_c$, $F^* - D^*$, $S_a - S_D$ assessing the capacity in terms of accelerations for both Nassar & Krawinkler and ADRS spectrum approaches. In Tables 7 and 8 the results, based on the ADRS spectrum the Nassar & Krawinkler formulation, are respectively reported.

**Table 7.** ADRS spectrum approach (SCBF).

| | FO | O | LS | NC |
|---|---|---|---|---|
| F [kN] | 3290.01 | 6009.54 | 6151.51 | 6107.34 |
| F* [kN] | 2340.99 | 4276.06 | 4377.08 | 4345.65 |
| d [m] | 0.0571 | 0.1171 | 0.1192 | 0.1867 |
| d* [m] | **0.0406** | **0.0833** | **0.0848** | **0.1328** |
| $S_a$* [g] | **0.2488** | **0.4545** | **0.4653** | **0.8151** |

**Table 8.** Nassar and Krawinkler approach (SCBF).

| | FO | O | LS | $NC_0$ |
|---|---|---|---|---|
| F [kN] | 3290.01 | 6009.54 | 6151.51 | 6229.56 |
| F* [kN] | 2340.99 | 4276.06 | 4377.08 | 4432.62 |
| d [m] | 0.0571 | 0.1171 | 0.1192 | 0.1867 |
| d* [m] | **0.0406** | **0.0833** | **0.0848** | **0.1328** |
| μ [m] | - | - | - | **1.566** |
| $S_a$* [g] | **0.2488** | **0.4545** | **0.6525** | **0.7399** |

Seismic performance verification requires that, for each limit state, the inequality $S_{a.SL}(T^*)_{capacity} \geq S_{a.SL}(T^*)_{demand}$ is satisfied.

### *5.3. Ordinary Concentrically Braced Frame*

Special concentrically braced frames are designed to fulfil the Eurocode 8 seismic provisions. The selected case study with the definition of the beam, diagonals, and column sections is reported in Figure 9.

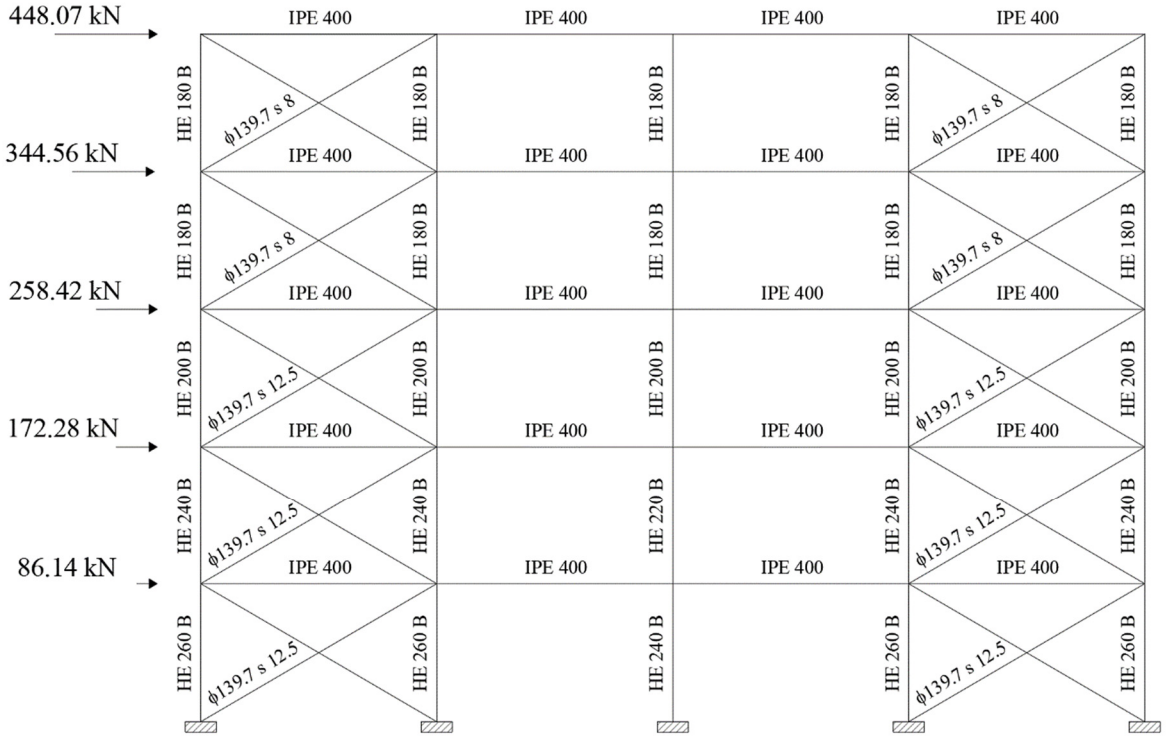


**Figure 9.** Diagram of the frame with indication of beams, diagonals, columns, and seismic forces (OCBF).

The trilinear capacity curve, showing the characteristic points of the model, is re-ported in Figure 10.

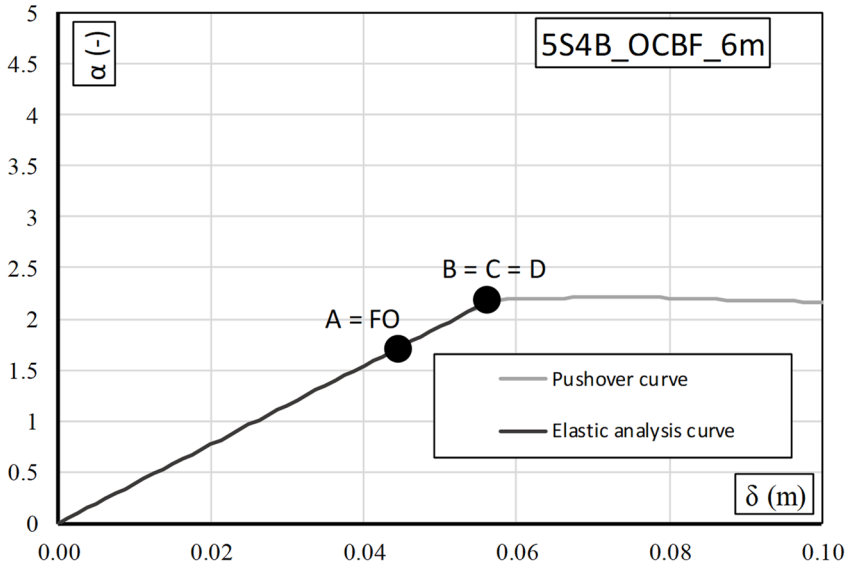


**Figure 10.** Trilinear model and characteristic points for the structure 5S4B_OCBF_6 m.

Parameters obtained from the elastic analysis:

- $\delta_1(\alpha = 1) = 0.02597$ m;
- $K$ =38.501 m$^{-1}$;
- $K' = 25.02$;
- $\delta_A$ =0.1602 m;
- $\alpha_A = k\delta_A$ =2.0680.

It is not necessary to perform rigid plastic analysis because the buckling of columns occurs for a multiplier of horizontal forces very close to $\alpha_A$. Consequently,

- $\delta_u = \delta_B = \delta_C = \delta_D = 0.0575\ m$;
- $\alpha_u = \alpha_B = \alpha_C = \alpha_D = 2.18596$.

The checking procedures exploit the transformation of the MDOF system into an equivalent SDOF system through the participation factor of the main vibration mode Γ. For this reason, it is necessary to define:

The eigenvector $\underline{\phi} = \{\phi_1, \phi_2, \phi_3, \phi_4, \phi_5\}$ that, assuming $\phi_k = \frac{F_k}{F_n}$, is:

$$\phi_1 = 0.192 \ \ \phi_2 = 0.384 \ \phi_3 = 0.575$$
$$\phi_4 = 0.767 \ \phi_5 = 1.00$$

The modal participation factor Γ:

$$\Gamma = \frac{\sum_{k=1}^{n} m_k \phi_k}{\sum_{k=1}^{n} m_k {\phi_k}^2} = 1.379$$

being

$$m_1 = 123.89 \times 10^3 \text{ kg } m_2 = 123.89 \times 10^3 \text{ kg } m_3 = 123.89 \times 10^3 \text{kg}$$
$$m_4 = 123.89 \times 10^3 \text{ kg } m_5 = 129.17 \times 10^3 \text{ kg}$$

and the dynamic parameters of the equivalent SDOF system (Table 9).

**Table 9.** Dynamic parameters of the equivalent SDOF system (OCBF).

| $m^*$ [kg $10^3$] | $k^*$ [kN/m] | $\omega^*$ [rad/s] | $T^*$ [s] |
|---|---|---|---|
| **366.82** | **37,127.6** | **10.061** | **0.6245** |

Therefore, the characteristic points of the capacity curve are defined in the planes $\alpha - \delta$, $F_b - d_c$, $F^* - D^*$, $S_a - S_D$ assessing the capacity in terms of accelerations for the Nassar and Krawinkler approach and ADRS spectrum approach. In particular, in Table 10, results based on the use of the ADRS spectrum, and, in Table 11, results based on the use of Nassar and Krawinkler formulation, are reported.

**Table 10.** ADRS spectrum approach (SCBF).

| | **FO** | **O** | **LS** | **NC** |
|---|---|---|---|---|
| F [kN] | 2235.76 | 2363.33 | 2363.33 | 2363.33 |
| F* [kN] | 1620.83 | 1713.31 | 1713.31 | 1713.31 |
| d [m] | 0.0538 | 0.0575 | 0.0575 | 0.0575 |
| d* [m] | **0.0390** | **0.0417** | **0.0417** | **0.0417** |
| $S_a$* [g] | **0.402** | **0.430** | **0.430** | **0.430** |

**Table 11.** Nassar and Krawinkler approach (SCBF).

| | **FO** | **O** | **LS** | **$NC_0$** |
|---|---|---|---|---|
| F [kN] | 2235.76 | 2363.33 | 2363.33 | 2363.33 |
| F* [kN] | 1620.83 | 1713.31 | 1713.31 | 1713.31 |
| d [m] | 0.0538 | 0.0575 | 0.0575 | 0.0575 |
| d* [m] | **0.0390** | **0.0417** | 0.0417 | 0.0417 |
| $\mu$ [m] | - | - | - | - |
| $S_a$* [g] | **0.450** | **0.476** | 0.476 | 0.476 |

Seismic performance verification requires that, for each limit state, the inequality $S_{a.SL}(T^*)_{capacity} \geq S_{a.SL}(T^*)_{demand}$ is satisfied.

## 6. Conclusions

In this paper, three numeric examples explaining the application of a new simplified assessment procedure for CBFs are reported. The given numerical examples show the speed and ease of application of the method, which is completely analytical. The equations of the branches constituting the trilinear model can be obtained uniquely, given the horizontal seismic actions and the sections of diagonals and columns of the analyzed frame. For this reason, this methodology is strongly suggested for the large-scale assessment of the seismic vulnerability of the built heritage. In addition, it constitutes a suitable tool for checking the capacity of the buildings designed with the new seismic code prescriptions, or for an evaluation of seismic vulnerability in the immediate aftermath of an earthquake. The reliability of the procedure is testified by an extensive regression analysis, carried out on 420 CBFs designed according to different approaches, belonging to different historical periods. In the sample cases, it is evident that the descending branch has an average slope like the one resulting from the pushover, while the difference in terms of the multiplier is due to the elastic deformability, which is not included in a rigid plastic model.

The feasibility of the procedure is very high and makes it suitable to be applied indiscriminately to frames belonging to different historical periods.

The scatter between the values computed from the pushover analysis and the proposed method of the maximum bearing multiplier $\alpha$ and the displacement corresponding to the collapse and formation of the plastic mechanism is usually lower than 10%, testifying the accuracy of the proposed formulations. In addition, the results achieved by the simplified assessment procedure are mainly on the safe side.

The assessment of structure vulnerability, in terms of a comparison of the capacity–demand, has also been performed by using the Nassar and Krawinkler approach, which is characterized by a wide generality because it does not discriminate between high and low periods of vibration and accounts for second-order effects.

It is important to mention that the code assessment approach does not provide the definition of specific performance points on the pushover curve. The user must identify target limits, which are provided by codes in terms of displacements. In the proposed methodology, on the other hand, specific limit states are also associated with performance points, making the capacity–demand comparison process immediate. The discretization of the trilinear model in characteristic points (A, B, C, D), associated with the achievement of predefined performance objectives, makes the comparison between the capacity and demand for each limit state given by codes easy.

**Author Contributions:** R.M.: conceptualization, methodology, writing—review and editing, supervision; E.N.: software, validation, resources, data curation, writing—review and editing, supervision; V.P.: conceptualization, methodology, writing—review and editing, supervision; P.T.: software, validation, writing—original draft, investigation, formal analysis. All authors have read and agreed to the published version of the manuscript.

**Funding:** The research leading to the results presented in this paper has received funding from the Italian Department of Civil Protection (DPC-Reluis).

**Institutional Review Board Statement:** Not applicable.

**Informed Consent Statement:** Not applicable.

**Acknowledgments:** The support of DPC-RELUIS 2019–2021 is gratefully acknowledged.

**Conflicts of Interest:** The authors declare no conflict of interest. The funders had no role in the design of the study; in the collection, analyses, or interpretation of data; in the writing of the manuscript, or in the decision to publish the results.

## Abbreviation

| Symbol | Description |
|---|---|
| $\alpha_y$ | Multiplier of horizontal forces corresponding to the formation of the first plastic hinge |
| $\alpha_{cr}$ | Critical multiplier for vertical loads |
| $\beta_{jk}$ | Inclination of the diagonal of k-th storey and j-th bay with respect to the horizontal direction |
| B | Inclination of the generic diagonal with respect to the horizontal direction |
| $\Gamma$ | Non-dimensional slope of the mechanism equilibrium curve |
| $\gamma_{ov}$ | Overstrength coefficient |
| $\delta_A$ | Top sway displacement corresponding to the minimum between the buckling of the first diagonal and the serviceability conditions—"Fully Operational" limit state |
| $\delta_B$ | Top sway displacement corresponding to the first yielding of a diagonal in tension—"Operational" limit state |
| $\delta_C$ | Top sway displacement corresponding to the maximum bearing capacity and the development of the collapse mechanism—"Life Safety" limit state |
| $\delta_D$ | Top sway displacement corresponding to the exceeding of at least one member of the local ductility supplies—"Near Collapse" limit state |
| $\delta_1$ | Elastic top sway displacement, corresponding to the design value of the seismic forces |
| $\delta_{d,cp}$ | Capacity of the diagonal members, in terms of elongation or compression, according to Eurocode 8 limitations |
| $1/\delta_1$ | Slope of the first elastic branch |
| $\delta_y = \delta_B$ | Top sway displacement corresponding to the yielding in tension of the first diagonal |
| $\delta_A$ | Top sway displacement corresponding to the buckling of the first diagonal |

| | |
|---|---|
| $\delta_{br}$ | Elongation or shortening of the generic diagonal member |
| $\delta_u$ | Ultimate top sway displacement |
| $\mu_{ls}$ | Ductility for the specific limit state |
| $\xi$ | Sensitivity coefficient for first storey members |
| $\phi_k$ | k-th component of the first mode eigenvector |
| $\varphi_{lim}$ | Capacity in terms of interstorey drift, defined according to Eurocode 8 limitations in terms of elongation or compression of the diagonal members |
| $\varphi$ | Stability coefficient |
| $A_{\dots}$ | Area of the generic member |
| a,b | Regression coefficients |
| E | Elastic modulus |
| $e_{t.jk} = e_{c.jk} = (h_k - h_{k-1}) \cdot \cos\beta_{jk}$ | Elongation of the tensile diagonal and the shortening of the compressed diagonal of j-th bay of k-th storey, given a unitary virtual rotation of the hinges at the base of the columns |
| $F_k$ | Design horizontal force applied at k-th storey |
| $F_{ls}$ | Base shear force corresponding to the specific limit state |
| $\varphi_{max}$ | Maximum interstorey drift |
| $\varphi_{lim}$ | Interstorey drift limit |
| $h_k$ | Storey height of k-th storey |
| $h_i$ | Interstorey height |
| $L_j$ | Bay span of the j-th bay |
| $L_{\dots}$ | Length of the generic member |
| $I_{\dots}$ | Moment of inertia of the generic member |
| $M_{c.ik}$ | Plastic moment of i-th column of k-th storey, reduced by the contemporaneous action of the axial force |
| $M_{pl}$ | Plastic resisting moment of the member |
| $N_{t.jk}$ | Yielding axial force of the tensile diagonal of j-th bay of k-th storey |
| $N_{c.jk}$ | Compressive axial force of the tensile diagonal of j-th bay of k-th storey accounting for the post-buckling behaviour according to Georgescu's model |
| $n_b$ | Number of bays |
| $n_c$ | Number of columns |
| $n_s$ | Number of storeys |
| $P_{crit}$ | Critical axial load defined according to Eurocode 3. |
| $P_y$ | Axial resistance in tension. |
| $q_{jk}$ | Vertical uniform load acting on the beam of j-th bay of k-th storey |
| q | Ratio between the maximum structural bearing capacity and the yielding capacity |
| $S_{a.ls}$ | Spectral acceleration in terms of capacity linked to the considered limit state |
| $S_a(T^*)$ | Spectral acceleration demand, provided by the code, for the specific limit state. |
| $V_k$ | Total vertical load acting on the k-th storey |
| $(\dots)^*$ | Properties referred to the equivalent SDOF system—m* (mass); T* (vibration period); ω* (pulse) |
| $W_{d.jk}$ | Internal work due to the diagonal braces of j-th bay of k-th storey, occurring for a unit virtual rotation of the hinges at the base of the columns |

## References


1. Jung, H.-C.; Jung, J.-S.; Lee, K.S. Seismic performance evaluation of internal steel frame connection method for seismic strengthening by cycling load test and nonlinear analysis. *J. Korea Concr. Inst.* **2019**, *31*, 79–88. [CrossRef]
2. Montuori, R.; Nastri, E.; Piluso, V. Problems of modeling for the analysis of the seismic vulnerability of existing buildings. *Ing. Sismica* **2019**, *36*, 53–85.
3. Montuori, R.; Nastri, E.; Piluso, V.; Todisco, P. A simplified performance-based approach for the evaluation of seismic performances of steel frames. *Eng. Struct.* **2020**, *224*, 111222. [CrossRef]
4. Montuori, R.; Nastri, E.; Piluso, V.; Todisco, P. Evaluation of the seismic capacity of existing moment resisting frames by a simplified approach: Examples and numerical application. *Appl. Sci.* **2021**, *11*, 2594. [CrossRef]
5. Balazadeh-Minouei, Y.; Tremblay, R.; Koboevic, S. Seismic Retrofit of an Existing 10-Story Chevron-Braced Steel-Frame. *J. Struct. Eng.* **2018**, *144*, 04018180. [CrossRef]
6. Nastri, E.; Vergato, M.; Latour, M. Performance evaluation of a seismic retrofitted R.C. precast industrial building. *Earthq. Struct.* **2017**, *12*, 13–21. [CrossRef]

7. Morelli, F.; Piscini, A.; Salvatore, W. Seismic behavior of an industrial steel structure retrofitted with self-centering hysteretic dampers. *J. Constr. Steel Res.* **2017**, *139*, 157–175. [CrossRef]
8. Wang, S.; Lai, J.-W.; Schoettler, M.J.; Mahin, S.A. Seismic assessment of existing tall buildings: A case study of a 35-story steel building with pre-Northridge connection. *Eng. Struct.* **2017**, *141*, 624–633. [CrossRef]
9. Hwang, S.-H.; Jeon, J.-S.; Lee, K. Evaluation of economic losses and collapse safety of steel moment frame buildings designed for risk categories II and IV. *Eng. Struct.* **2019**, *201*, 10983. [CrossRef]
10. Seker, O.; Faytarouni, M.; Akbas, B.; Shen, J. A novel performance-enhancing technique for concentrically braced frames incorporating square HSS. *Eng. Struct.* **2019**, *201*, 109800. [CrossRef]
11. Taiyari, F.; Formisano, A.; Mazzolani, F.M. Seismic Behaviour Assessment of Steel Moment Resisting Frames under Near-Field Earthquakes. *Int. J. Steel Struct.* **2019**, *19*, 1421–1430. [CrossRef]
12. Bojórquez, E.; López-Barraza, A.; Reyes-Salazar, A.; Ruiz, S.E.; Ruiz-García, J.; Formisano, A.; López-Almansa, F.; Carrillo, J.; Bojórquez, J. Improving the Structural Reliability of Steel Frames Using Posttensioned Connections. *Adv. Civ. Eng.* **2019**, *2019*, 8912390. [CrossRef]
13. Terracciano, G.; Di Lorenzo, G.; Formisano, A.; Landolfo, R. Cold-formed thin-walled steel structures as vertical addition and energetic retrofitting systems of existing masonry buildings. *Eur. J. Environ. Civ. Eng.* **2015**, *19*, 850–866. [CrossRef]
14. Formisano, A.; Landolfo, R.; Mazzolani, F.M. Robustness assessment approaches for steel framed structures under catastrophic events. *Comput. Struct.* **2015**, *147*, 216–228. [CrossRef]
15. Mangalathu, S.; Hwang, S.-H.; Choi, E.; Jeon, J.-S. Rapid seismic damage evaluation of bridge portfolios using machine learning techniques. *Eng. Struct.* **2019**, *201*, 109785. [CrossRef]
16. Krawinkler, H.; Seneviratna, G.D.P.K. Pros and cons of a pushover analysis of seismic performance evaluation. *Eng. Struct.* **1998**, *20*, 452–464. [CrossRef]
17. Brebbia, C. *Earthquake Resistant Engineering Structures X, WIT Transactions on the Built Environment*; Technology & Engineering; WIT Press: Southampton, UK, 2015.
18. Gupta, A.; Krawinkler, H. Feasibility of push-over analyses for estimation of strength demand, Stessa 2003—Behaviour of Steel Structures in Seismic Areas. In Proceedings of the 4th International Specialty Conference, Naples, Italy, 9–12 June 2003.
19. NTC 2018 Italian Code: Chapter 7 "Design for seismic actions".
20. Fajfar, P. A Nonlinear Analysis Method for Performance-Based Seismic Design. *Earthq. Spectra* **2000**, *16*, 573–592. [CrossRef]
21. Gentile, R.; del Vecchio, C.; Pampanin, S.; Raffaele, D.; Uva, G. Refinement and Validation of the Simple Lateral Mechanism Analysis (SLaMA) Procedure for RC Frames. *J. Earthq. Eng.* **2021**, *25*, 1227–1255. [CrossRef]
22. Bernuzzi, C.; Rodigari, D.; Simoncelli, M. Post-earthquake damage assessment of moment resisting steel frames. *Ing. Sismica* **2019**, *36*, 35–55.
23. Costanzo, S.; D'Aniello, M.; Landolfo, R. Seismic design rules for ductile Eurocode compliant two storey X concentrically braced frames. *Steel Compos. Struct.* **2020**, *36*, 273–291. [CrossRef]
24. Costanzo, S.; Tartaglia, R.; Di Lorenzo, G.; De Martino, A. Seismic Behaviour of EC8-Compliant Moment Resisting and Concentrically Braced Frame. *Buildings* **2019**, *9*, 196. [CrossRef]
25. Costanzo, S.; D'Aniello, M.; Landolfo, R. The influence of moment resisting beam-to-column connections on seismic behavior of chevron concentrically braced frames. *Soil Dyn. Earthq. Eng.* **2018**, *113*, 136147. [CrossRef]
26. Costanzo, S.; D'Aniello, M.; Landolfo, R. Seismic design criteria for chevron CBFs: European vs. North American codes (part-1). *J. Constr. Steel Res.* **2017**, *135*, 83–96. [CrossRef]
27. Costanzo, S.; D'Aniello, M.; Landolfo, R.; De Martino, A. Critical discussion on seismic design criteria for cross concentrically braced frames. *Ing. Sismica Int. J. Earthq. Eng.* **2018**, *35*, 23–36.
28. Karamanci, E.; Lignos, D.G. Computational Approach for Collapse Assessment of Concentrically Braced Frames in Seismic Regions. *J. Struct. Eng.* **2014**, *140*, A4014019. [CrossRef]
29. Pengfei, W.; Shan, G.; Sheling, W.; Xiaofei, W. Anti-collapse equivalent dynamic analysis on steel moment frame. *Ing. Sismica* **2019**, *36*, 1–19.
30. Ferraioli, M.; Lavino, A.; Mandara, A. Effectiveness of multi-mode pushover analysis procedure for the estimation of seismic demands of steel moment frames. *Ing. Sismica* **2018**, *35*, 78–90.
31. Bernuzzi, C.; Chesi, C.; Rodigari, D.; De Col, R. Remarks on the approaches for seismic design of moment-resisting steel frames. *Ing. Sismica* **2018**, *35*, 37–47.
32. Pongiglione, M.; Calderini, C.; D'Aniello, M.; Landolfo, R. Novel reversible seismic-resistant joint for sustainable and deconstructable steel structures. *J. Build. Eng.* **2021**, *35*, 101989. [CrossRef]
33. Formisano, A.; Massimilla, A.; Di Lorenzo, G.; Landolfo, R. Seismic retrofit of gravity load designed RC buildings using external steel concentric bracing systems. *Eng. Fail. Anal.* **2020**, *111*, 104485. [CrossRef]
34. Di Lorenzo, G.; Colacurcio, E.; Di Filippo, A.; Formisano, A.; Massimilla, A.; Landolfo, R. State-of-the-art on steel exoskeletons for seismic retrofit of existing RC buildings. *Ing. Sismica* **2020**, *37*, 33–50.
35. Romano, E.; Cascini, L.; D'Aniello, M.; Portioli, F.; Landolfo, R. A simplified multi-performance approach to life-cycle assessment of steel structures. *Structures* **2020**, *27*, 371–382. [CrossRef]
36. Montuori, R.; Nastri, E.; Piluso, V.; Todisco, P. Performance-based rules for the simplified assessment of steel CBFS. *J. Constr. Steel Res.* **2022**, *191*, 107167. [CrossRef]

37. Gupta, A.; Krawinkler, H. *Seismic Demands for Performance Evaluation of Steel Moment Resisting Frame Structures*; Stanford University: Stanford, CA, USA, 1999.
38. Bruneau, M.; Uang, C.M.; Sabelli, R.S.E. *Ductile Design of Steel Structures*, 2nd ed.; McGraw-Hill: New York, NY, USA, 2011.
39. Eurocode 8. EN 1998-3: Design of Structures for Earthquake Resistance—Part 3: Assessment and Retrofitting of Buildings, CEN. 2004. Available online: https://www.phd.eng.br/wp-content/uploads/2014/07/en.1998.3.2005.pdf (accessed on 26 January 2022).
40. Nassar, A.A.; Krawinkler, H. *Seismic Demands for SDOF and MDOF Systems. John A Blume Earthquake Engineering Center Technical Report 95*; Stanford Digital Repository: Stanford, CA, USA, 1991.
41. Montuori, R.; Nastri, E.; Piluso, V. Advances in theory of plastic mechanism control: Closed form solution for MR-Frames. *Earthq. Eng. Struct. Dyn.* **2015**, *44*, 1035–1054. [CrossRef]
42. Longo, A.; Montuori, R.; Piluso, V. Moment frames—Concentrically braced frames dual systems: Analysis of different design criteria. *Struct. Infrastruct. Eng.* **2016**, *12*, 122–141. [CrossRef]
43. Nastri, E.; D'Aniello, M.; Zimbru, M.; Streppone, S.; Landolfo, R.; Montuori, R.; Piluso, V. Seismic response of steel Moment Resisting Frames equipped with friction beam-to-column joints. *Soil Dyn. Earthq. Eng.* **2019**, *119*, 144–157. [CrossRef]
44. Piluso, V.; Montuori, R.; Nastri, E.; Paciello, A. Seismic response of MRF-CBF dual systems equipped with low damage friction connections. *J. Constr. Steel Res.* **2019**, *154*, 263–277. [CrossRef]
45. Krishnan, S.; Muto, M. Mechanism of collapse of Tall Steel Moment-Frame Buildings under Earthquake Excitation. *J. Struct. Eng.* **2012**, *138*, 1361–1387. [CrossRef]
46. Piluso, V.; Pisapia, A.; Castaldo, P.; Nastri, E. Probabilistic Theory of Plastic Mechanism Control for Steel Moment Resisting Frames. *Struct. Saf.* **2019**, *76*, 95–107. [CrossRef]
47. Priestley, M.J.N. Performance based seismic design. *Bull. N. Z. Soc. Earthq. Eng.* **2000**, *33*, 325–346. [CrossRef]
48. Bruneau, M.; Uang, C.M.; Whittaker, A. *Ductile Design of Steel Structures*; McGraw-Hill: New York, NY, USA, 1998.
49. Georgescu, D.; Toma, C.; Gosa, O. Post-critical Behaviour of "K"Braced Frames. *J. Constr. Steel Res.* **1992**, *21*, 115–133. [CrossRef]
50. Eurocode 8. EN 1998-1: Design of Structures for Earthquake Resistance—Part 1: General Rules, Seismic Actions and Rules for Buildings, CEN. 2004. Available online: https://www.phd.eng.br/wp-content/uploads/2015/02/en.1998.1.2004.pdf (accessed on 26 January 2022).
51. Eurocode 3. UNI EN 1993-1-1: Design of Steel Structures Part 1-1: General Rules and Rules for Buildings, CEN. 2005. Available online: https://www.phd.eng.br/wp-content/uploads/2015/12/en.1993.1.1.2005.pdf (accessed on 26 January 2022).
52. Mazzolani, F.M.; Piluso, V. Plastic Design of Seismic Resistant Steel Frames. *Earthq. Eng. Struct. Dyn.* **1997**, *26*, 167–191. [CrossRef]
53. Mazzolani, F.M.; Piluso, V. *Theory and Design of Seismic Resistant Steel Frames*; E & FN Spon: London, UK, 1996.
54. Yun, S.Y.; Hamburger, R.O.; Cornell, C.A.; Foutch, D.A. Seismic performance evaluation for steel moment frames. *J. Struct. Eng.* **2002**, *128*, 534–545. [CrossRef]
55. Grecea, D.; Dinu, F.; Dubina, D. Performance Criteria for MR Steel Frames in Seismic Zones. *J. Constr. Steel Res.* **2004**, *60*, 739–749. [CrossRef]
56. Newmark, N.; Hall, W. Earthquake Spectra and Design. In *EERI Monographs*; Earthquake Engin. Research Library: Richmond, CA, USA, 1982.
57. Ferraioli, M.; Lavino, A.; Mandara, A. An adaptive capacity spectrum method for estimating seismic response of steel moment-resisting frames. *Ing. Sismica* **2016**, *33*, 47–60.
58. Naeim, F. Earthquake Engineering-From Engineering Seismology to Performance-Based Engineering. *Earthq. Spectra* **2005**, *21*, 609–611. [CrossRef]